Formation of casein micelles from bovine caseins simulating human casein phosphorylation patterns : Micellar structure and in vitro infant gastrointestinal digestion

Food Hydrocolloids

Yang, Tingting; Hong, Xinhuizi; Tao, Xiumei; Zhang, Jielong; Liu, Dasong et al

https://doi.org/10.1016/j.foodhyd.2024.110020

Food Hydrocolloids 153 (2024) 110020

Contents lists available at ScienceDirect

Food Hydrocolloids

journal homepage: www.elsevier.com/locate/foodhyd

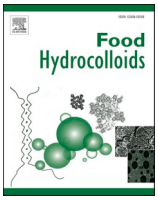

Formation of casein micelles from bovine caseins simulating human casein phosphorylation patterns: Micellar structure and *in vitro* infant gastrointestinal digestion

Tingting Yang [a,b], Xinhuizi Hong [a,b], Xiumei Tao [a,c], Jielong Zhang [a,b], Dasong Liu [a,b,*], Xiaoming Liu [a,b], Thom Huppertz [d,e], Joe M. Regenstein [f], Peng Zhou [a,b]

[a] State Key Laboratory of Food Science and Resources, Jiangnan University, Wuxi, Jiangsu Province, 214122, China
[b] School of Food Science and Technology, Jiangnan University, Wuxi, Jiangsu Province, 214122, China
[c] Analysis and Testing Center, Jiangnan University, Wuxi, Jiangsu Province, 214122, China
[d] Food Quality and Design Group, Wageningen University & Research, Wageningen, the Netherlands
[e] FrieslandCampina, Amersfoort, the Netherlands
[f] Department of Food Science, Cornell University, Ithaca, NY, 14853-7201, USA

ARTICLE INFO

Keywords:
Casein dephosphorylation
Micelles
Infants
Bovine milk
Human milk

ABSTRACT

This study investigated the micellar structure and *in vitro* infant gastrointestinal digestion of formed casein micelles simulating human casein composition and phosphorylation patterns. Caseins were fractionated from bovine caseins and formulated according to human casein composition, i.e., β-, κ- and α_{s1}-caseins with a ratio of 68:20:12. The formulated caseins were dephosphorylated for different times and were mixed to obtain mixed phosphorylation patterns (FC-MP) for β-casein, showing 0–5 phosphate groups comparable to human β-casein. The formulated caseins without dephosphorylation and with high dephosphorylation, showing 5 phosphate groups and 0–2 phosphate groups for β-casein, respectively, were categorized as high (FC-HP) and low phosphorylated (FC-LP). With the average mineral concentrations found in human milk, $CaCl_2$, $MgCl_2$, citrate and inorganic phosphate were added into the different formulated casein dispersions to obtain casein micelles (FM-HP, FM-MP and FM-LP). Compared to FM-HP, FM-MP was closer to human micelles in relation to particle size, micellar hydration, molar ratio of Ca:casein, morphology and internal structure, whereas FM-LP showed did not show a characteristic micellar structure and had a larger size and lower molar ratio of Ca:casein. For gastrointestinal digestion, FM-MP was closer to human micelles in terms of the gastric flocs, casein degradation rate, free amino groups, and molecular weight distribution of peptides compared to FM-HP, whereas FM-LP showed larger flocs and lower casein degradation rate. These results show the significance of post-translational phosphorylation in facilitating the assembly of caseins into micellar structures, indicating the potential to form human-like micelles for application in infant formulae.

1. Introduction

Proteins in infant formulae are predominantly from bovine milk. Bovine casein micelles show variations from human casein micelles in caseins' composition, phosphorylation patterns and structure (Meng, Uniacke-Lowe, Ryan, & Kelly, 2021). Bovine micelles consist of α_{s1}-casein, α_{s2}-casein, β-casein, and κ-casein in a ratio of 4:1:3.5:1.5, while human micelles are composed of α_{s1}-casein, β-casein, and κ-casein in a ratio of 12:68:20, with no detectable α_{s2}-casein (Roy, Ye, Moughan, & Singh, 2020). The β-casein and α_{s1}-casein in bovine micelles were found as phosphorylated isoforms with 5 and 8–9 phosphate groups (5-P; 8-9-P), respectively, while β-casein and α_{s1}-casein occur in human micelles with mixed phosphorylated isoforms having 0–5 and 0–8 phosphate groups, respectively (Poth, Deeth, Alewood, & Holland, 2008). The internal structure of micelles is formed via casein-casein associations and ionic bonds of colloidal Ca towards phosphate groups of caseins (Antuma, Steiner, Garamus, Boom, & Keppler, 2023; Dalgleish & Corredig, 2012). Bovine casein micelles have a higher mineralization, larger size, and denser structure compared to human micelles (Huppertz & Timmer, 2020; Meng et al., 2021). These differences could result in an

* Corresponding author. State Key Laboratory of Food Science and Resources, Jiangnan University, Wuxi, Jiangsu Province, 214122, China.
E-mail address: liudasong68@163.com (D. Liu).

https://doi.org/10.1016/j.foodhyd.2024.110020
Received 31 December 2023; Received in revised form 17 March 2024; Accepted 20 March 2024
Available online 27 March 2024

inferior digestibility and absorption of bovine milk-based infant formula compared to human milk, which might affect the growth and development of formula-fed infants (Berton et al., 2012; Roy et al., 2020).

Previous research has shown the enzymatic dephosphorylation of fractionated caseins, caseinates and bovine casein micelles to simulate the degree of phosphorylation of human caseins, as well as their corresponding effects on gastrointestinal digestion (Power, Fenelon, O'Mahony, & McCarthy, 2019; Song, Lin, Zhang, Luo, & Guo, 2023). Li-Chan and Nakai (1989) reported that 99% and 27% dephosphorylation were achieved for isoelectric bovine whole caseins and bovine casein micelles, respectively, after treatment with potato acid phosphatase. The *in vitro* gastric digestibility of the dephosphorylated caseins was higher compared to that of the untreated bovine caseins. Liu et al. (2016) reported that bovine casein micelles treated with calf intestinal alkaline phosphatase produced dephosphorylated caseins with a degree of dephosphorylation of up to 42%. The β-casein isoforms had 0-2 phosphate groups, and the dephosphorylated caseins had looser gastric clots and faster degradation using an infant *in vitro* gastrointestinal digestion model (Liu et al., 2016). However, limited information is currently available regarding simulating the mixed phosphorylation patterns of human caseins by dephosphorylation of bovine caseins.

Casein micelles have been formed to simulate the original micellar structures by cautiously mixing mineral solutions with a casein solution or by concentrating a dilute solution of minerals and caseins or by increasing pH of an acidic solution of minerals and caseins (Antuma et al., 2024; Hemar, Xu, Wu, & Ashokkumar, 2020). These previous researches mainly focused on the effects of mineral compositions and concentrations, casein compositions and concentrations, casein dephosphorylation degrees, solution mixing approaches, and extrinsic factors such as temperature and pH on the structures and functionalities of the formed micelles (Antuma et al., 2023; Sood, Lekic, Jhawar, Farrell, & Slattery, 2006). Sood, Erickson, and Slattery (2005) reported that a human β-casein mixture consisting of the 0-P, 1-P, 2-P, 3-P, 4-P and 5-P isoforms at a ratio of 5:8:26:15:33:13 was mixed with bovine κ-casein at a κ-casein/β-casein molar ratio of 0.33, with added Ca and P_i to induce the formation of casein micelles. However, limited information is available regarding the formation process for those casein micelles that strongly simulate human micelles with regard to casein compositions, phosphorylation patterns, mineral compositions and internal structures. There is even less understanding regarding the gastrointestinal digestion patterns of these simulated human micelles.

Previously, casein micelles were formed to simulate human caseins and their mineral compositions (Yang et al., 2024). The size, hydration, morphology and the gastric flocs were close to human micelles, whereas the molar ratio of Ca:casein was higher and the rate of casein degradation was lower than human micelles (Yang et al., 2024). This might be due to human β-casein having mixed phosphorylation patterns that were predominated by the isoforms of 0-P, 1-P, 2-P and 4-P (Poth et al., 2008), which was difficult to simulate by controlling the conditions for enzymatic dephosphorylation of the bovine counterpart. Therefore, this study focused on obtaining formulated caseins similar to human casein composition, and then to simulate the phosphorylation patterns of human caseins by mixing formulated caseins dephosphorylated for different times. This was followed by adding minerals to induce the development of casein micelles. The study assessed the microstructures and *in vitro* gastrointestinal digestibility with infant appropriate conditions for the modified casein micelles, aiming to prepare bovine-derived infant formula designed to more closely simulate human milk.

2. Materials and methods

2.1. Materials

Fresh bovine milk was obtained from Tianzi Dairy Co., Ltd. (Wuxi, Jiangsu, China). Human milk was sourced from 10 healthy donors at 2–8 months postpartum, with authorization from the Medical Ethics Committee of Jiangnan University (certificate number JNU20220606IRB10). Bovine and human milk were skimmed at 3000×*g* for 30 min at 25 °C using a Soryall LYNX 4000 centrifuge (Themo Electron LED GmbH, Osterode, Germany). The human skim milk was ultracentrifuged at 150,000×*g* for 60 min utilizing an Optima L-100XP ultracentrifuge (Beckman Coulter, Inc., Indianapolis, IN, USA). The supernatant was further processed using centrifugal ultrafiltration at 2500×*g* for 60 min utilizing a Vivaspin 6 concentrator (Sartorius Stedim Biotech GmbH, Goettingen, Germany) featuring a nominal 10 kDa molecular weight cut-off filter. The precipitate was dissolved in the respective ultrafiltrate to obtain 0.4% (w/v) human casein micelle dispersions (Hailu et al., 2016). Calf intestinal alkaline phosphatase (10 U/mg), porcine gastric mucosa pepsin (3880 U/mg), pepstatin A, fluorescein isothiocyanate isomer I, porcine pancreatin (7.4 U/mg), Pefabloc® SC and o-phthaldialdehyde (OPA) were obtained from Sigma-Aldrich Co. (St. Louis, MO, USA). All other chemicals were at least of analytical grade and mainly obtained from Sinopharm Chemical Reagent Co., Ltd. (Shanghai, China).

2.2. Fractionation and formulation of caseins

Bovine skim milk was mixed with 2 M HCl to pH 4.6 and centrifuged at 10,000×*g* at 25 °C using an Avanti centrifuge (Beckman Coulter) for 15 min to obtain precipitated caseins. The precipitate was redissolved in ultrapure water (Heal Force Water Purification System, Canrex Analytic Instrument Co., Ltd., Shanghai, China) to obtain dispersions at 2.5% (w/v). The casein dispersion was adjusted to pH 11 using 2 M NaOH and then 0.65 M CaCl2 was added to obtain a final concentration of 65 mM Ca. After adding 2 M HCl to reach pH 7.0, the dispersion was centrifuged at 10,000×*g* for 15 min (Thienel et al., 2018).

The supernatant was mixed with 6 M HCl to pH 3.8, and centrifuged at 10,000×*g* for 15 min to achieve a κ-casein-enriched fraction, whereas the precipitate was redissolved in ultrapure water at a casein concentration of 2.5% (w/v) and adjusted to pH 7.0 using 2 M NaOH. The casein dispersion was kept at 4 °C for 6 h and then adjusted to pH 4.6 using 2 M HCl. It was centrifuged at 4 °C at 10,000×*g* for 15 min, and the supernatant was incubated at 30–35 °C for 30 min, followed by centrifugation at 10,000×*g* for 15 min to obtain the precipitate as a β-casein fraction (Post, Arnold, Weiss, & Hinrichs, 2012).

The κ-casein and β-casein fractions were dissolved in ultrapure water and subjected to dialysis against ultrapure water at 4 °C, using tubing with a nominal molecular weight cut-off of 7 kDa (Shanghai Green Bird Science and Technology Development Co., Shanghai, China). Subsequently, lyophilization was carried out utilizing a BenchTop Pro freeze drier (SP Scientific Co., Stone Ridge, NY, USA). Freeze-dried samples were stored at −80 °C for a maximum of 10 wk. The bovine caseins with compositions similar to those found in human caseins were obtained by mixing the κ-casein and β-casein with a ratio of 10:7 (w/w). The κ-casein-enriched fraction comprised β-casein, κ-casein and α_{s1}-caseins in a ratio of 44:36:20, whereas the β-casein fraction contained negligible amounts of α_{s1}-casein, α_{s2}-casein, and κ-casein.

2.3. Modification of casein phosphorylation patterns

Formulated caseins were dephosphorylated using calf intestinal alkaline phosphatase following the methodology of Liu et al. (2019). Briefly, the caseins (5 mg/mL, pH 8.0) were dissolved in ultrapure water, and intestinal alkaline phosphatase was dissolved in 50 mM Tris-HCl buffer (pH 8.0). The casein dispersion was mixed with an equal volume of phosphatase solution (0.4 U/mL) and subsequently kept at 37 °C for up to 420 min. At predetermined intervals, samples were withdrawn for analysis. The reaction was terminated by heating at 80 °C for 10 min before adjusting pH to 6.7 with 1 M HCl. The solutions of dephosphorylated caseins after 1, 15 and 180 min were mixed at a volume ratio of 1:2:0.4 to obtain formulated caseins with mixed phosphorylation patterns (FC-MP). The solutions of formulated caseins

dephosphorylated for 0 and 180 min were used for the samples with high phosphorylated (FC-HP) and low phosphorylation patterns (FC-LP), respectively. These solutions were dialyzed against ultrapure water at a ratio of 1:50 (sample to water) at 4 °C using the aforementioned 7 kDa dialysis tubing and then lyophilized.

2.4. Formation of casein micelles

Casein micelles were formed following the methodology of Hemar et al. (2020). In brief, FC-HP, FC-MP and FC-LP (Section 2.3) were dissolved in ultrapure water to obtain a casein concentration of 0.8% (w/v). Stock solutions of $CaCl_2$ (41.0 mM for FC-HP, 41.2 mM for FC-MP, 42.2 mM FC-LP) plus $MgCl_2$ (10 mM), $C_6H_5K_3O_7$ (Cit, 230 mM) and K_2HPO_4 (P_i, 18.6 mM) were prepared. Each dispersion (10 mL) was put into a 25 mL jacketed glass beaker maintained at 37 °C. Stock solutions of $CaCl_2$:$MgCl_2$ at a mole ratio of Ca:Mg of 7.1:1.5 (3 mL), Cit (200 μL) and P_i (3 mL) were slowly added dropwise sequentially into the beaker with magnetic stirring, followed by adjusting the pH to 7.0 using 1 M HCl. The final volume was adjusted to 20 mL using ultrapure water. The three samples of formed casein micelles were obtained (FM-HP, FM-MP and FM-LP). The final concentrations of caseins, Ca, Mg, Cit and P_i in the micelle dispersions were 0.4%, 7.1, 1.5, 2.3 and 2.8 mM, respectively.

To investigate the effect of mineral concentration, varied concentrations of Ca stock solutions at a Ca:Mg molar ratio of 7.1:1.5 were prepared, where the concentrations of Ca stock solutions were 6.7–67.7 mM for FC-HP, 7.7–68.7 mM for FC-MP, and 8.7–69.7 mM for FC-LP and those of Mg were 3.0–15.6 mM. Optical absorbance of the dispersions was determined using an UV-2700 spectrophotometer (Shimadzu Corp., Kyoto, Japan) at 400 nm.

2.5. In vitro digestion in an infant model

The infant *in vitro* gastrointestinal model digestion, which was done at a higher pH than for adults, followed the method of Ménard et al. (2018) with minor modifications. According to Ménard et al. (2018), this method was developed based on *in vivo* relevant parameters such as meal to secretions ratio, emptying half time and pH derived from the gastrointestinal tract of full-term newborn aged ~1 month (Bourlieu et al., 2014; Minekus et al., 2014). The enzymatic activities of porcine pepsin and pancreatin were measured according to Brodkorb et al. (2019). To simulate gastric digestion, the micelles were mixed with simulated gastric fluid at a ratio of 63:37 (724 U pepsin/mL gastric fluid, pH 5.3, 94 mM NaCl, 13 mM KCl), followed by resetting the pH to 5.3 using 1 M HCl. Following gastric digestion, the digesta were adjusted to pH 7.0 by gradually adding 2 M NaOH, followed by mixing in a ratio of 62:38 (v/v) with intestinal fluid (pH 6.6, containing 42 U/mL intestinal fluid, 249 mM NaCl, 10 mM KCl, 3.1 mM bile salt, with pH then adjusted to 6.6 using 1 M HCl.

Gastrointestinal digestion was done at 37 °C. Digesta samples were collected at 0, 1, 3, 6, 10, 20, 30 and 60 min during both the gastric and intestinal digestion, and 7.3 μM pepstatin A or 5.0 mM Pefabloc® SC were added to terminate digestion. The control sample, devoid of pepsin, was represented by the digesta collected at 0 min. Gastric digesta (2 mL) was deposited into a Petri dish and captured using a camera (Canon Inc., Tokyo, Japan).

2.6. Analytical methods

2.6.1. Urea-polyacrylamide gel electrophoresis (Urea-PAGE)

To identify the phosphorylation patterns of caseins, urea-PAGE was done with a PROTEAN II XL Cell system (Bio-Rad Laboratories, Inc., Hercules, CA, USA), using a 4% stacking gel and an 8% resolving gel made following the method of Bansal, Fox, and Mcsweeney (2007). The formulated casein dispersions with different phosphorylation patterns (Section 2.3) and human milk were mixed with sample buffer (pH 7.6, containing 50 mM Tris-HCl, 8 M urea and 5% (v/v) β-mercaptoethanol) at a mixing ratio of sample to buffer of 1:1 (v/v). The voltages were 280 V for the stacking gel and 300 V for the resolving gel. Following electrophoresis, the gels were immersed in a staining solution of 0.1% (w/v) Coomassie Brilliant Blue G-250 in 1 M H_2SO_4 for 4 h and de-stained using water until clear bands could be identified. Semi-quantitative analysis of the band intensity was done utilizing Image Lab™ 3.0 software (Bio-Rad Laboratories) assuming bands were in the Beer-Lambert's Law region. The assignment of each band was done according to Andrews (1983).

2.6.2. Ultra-performance liquid chromatography-electrospray ionization-mass spectrometry (UPLC-ESI-MS)

The dispersions with different phosphorylation patterns and human milk were mixed with buffer (pH 7.0) containing 8 M urea, 0.1 M Bis-Tris propane, 1.3% (w/v) trisodium citrate dihydrate and 20 mM dithiothreitol. The mixing ratio of the sample to buffer was 1:1 (v/v). An UPLC-ESI-MS system (Platform ZMD 4000, Waters Co., Milford, MA, USA) equipped with an ethylene-bridged hybrid C4 column (100 × 2.1 mm I.D., Waters) was used to analyze the filtrate following Semagoto et al. (2014) with minor adjustments. Mobile phases included Solution A (0.1% formic acid in water) and Solution B (100% acetonitrile). Elution was carried out at a flow rate of 0.3 mL/min utilizing a linear gradient from 10 to 90% B within 30 min. Mass measurements were done using the positive ionization mode. The cone-hole voltage was set at 40 V, while the collision energy was 6 eV. MS spectra were acquired within the 500–3000 m/z range, using a scan time of 1 s with an interval of 0.02 s. Data analysis was done utilizing MassLynx V4.1 and MassEnt1 software (Waters).

2.6.3. Determination of minerals and caseins

The formed micelle dispersions were ultracentrifuged at 150,000×*g* at 25 °C for 1 h. For determination of Ca concentrations, the dispersions and their supernatants were hydrolyzed using nitric-perchloric acid (4:1, v/v) with a MARS Microwave Digestion System (CEM Corp., Matthews, NC, USA). Total and serum Ca levels were subsequently measured using an iCAP TQ ICP-MS (Thermo Fisher Scientific, Inc., Bremen, Germany), following the method of ISO (2018). The difference between the total and serum Ca corresponded to the colloidal Ca. Human milk and the formulated casein dispersions were hydrolyzed as above, and the concentrations of Ca and Mg were also determined using the ICP-MS. A multi-element standard solution (Agilent Technology Inc., Santa Clara, CA, USA) was used as the standard.

To determine P_i and Cit, the casein dispersions and human skim milk were mixed 1:1 (v/v) with 30% (w/v) trichloroacetic acid (TCA) and subsequently centrifuged at 10,000×*g* for 60 min. The concentrations of Cit and P_i in the supernatants were quantified using the RP-HPLC and the ICP-MS, respectively, following Garnsworthy, Masson, Lock, and Mottram (2006) and ISO (2018). An e2695 Separations Module (Waters) fitted with a Waters Symmetry C18 column (250 × 4.6 mm I.D.) with a detector set at 218 nm was used. The mobile phase was 98% 0.1 M KH_2PO_4 (pH 3.0 with H_3PO_4 + 2% acetonitrile) and flow rate was 1.0 mL/min.

The protein content in both the micelle dispersions and their supernatants was determined using the method of ISO (2001) with a K1302 Kjeldahl unit (Sonnen Automated Analysis Instrument Co., Ltd., Shanghai, China) for total and serum caseins. The difference between the total caseins and serum caseins was the micellar caseins.

To assess casein composition, the dispersions and their supernatants were mixed with an equal volume of the buffer described in Section 2.6.2. The mixture was then subjected to analysis utilizing the RP-HPLC system equipped with a Waters 2489 UV/Visible detector and a Zorbax 300SB C8 column (250 × 4.6 mm I.D.; Agilent Technologies) according to Yang, Liu, and Zhou (2022). The mobile phases were Solvent A (acetonitrile-water-trifluoroacetic acid, 100:900:1, v/v/v) and solvent B (acetonitrile-water-trifluoroacetic acid, 900:100:0.7, v/v/v). Elution

was done at a flow rate of 0.8 mL/min, starting with a gradient from 26 to 44% B within 55 min, then increasing to 70% B in the subsequent 2 min and maintaining that level for 3 min. Subsequently, returning to 26% B within 2 min and maintaining it for 3 min. The column temperature was maintained at 30 °C, and the detection wavelength was set at 220 nm. The percentage of each casein was calculated based on its peak area relative to the total peak area of all caseins, assuming uniform detector response across all peaks.

2.6.4. Dynamic light scattering (DLS)

To measure the size of micelle dispersions, DLS was done using an ALV/CGS-3 (ALV-GmbH, Langen, Germany) as previously described by Pitkowski, Nicolai, and Durand (2008). A refractive index of 1.57 had been established for casein particles in solution using a scattering angle of 90° at a wavelength of 633 nm (Liu & Guo, 2008). Data analysis was done using the ALV-7004 Correlator software.

2.6.5. Determination of micellar hydration

To determine micellar hydration, the casein micelle dispersions were centrifuged at 150,000×*g* at 25 °C for 1 h. The resultant precipitate was oven-dried at 105 °C for 7–8 h. The difference in weights pre- and post-drying, expressed as g water/g dry matter, was considered indicative of micellar hydration.

2.6.6. Cryo-transmission electron microscopy (Cryo-TEM) and atomic force microscopy (AFM)

Cryo-TEM was done using a Talos F200C cryo-transmission electron microscope (Thermo Fisher Scientific, Inc., Hillsboro, OR, USA) according to Wu et al. (2020). Casein micelle dispersions (3–5 μL) were placed onto a lacey carbon film (200 mesh, 50 nm pore diameter; Sigma-Aldrich) supported by a copper grid. The excess liquid was carefully removed by blotting with filter paper (9.6 cm^2 surface area; Sinopharm Chemical Reagent), resulting in a thin liquid film. Subsequently, the copper grid was rapidly submerged into −170 °C liquid ethane for rapid freezing.

AFM analysis was done using a Dimension Icon atomic force microscope (Brock Technology Co., Ltd., Billerica, MA, USA) following Ouanezar, Guyomarc'h, and Bouchoux (2012). Dispersions (3–5 μL) were carefully deposited onto a pristine mica surface sheet (15 × 15 mm; Head Biotechnology Co., Ltd, Beijing, China) and subsequently air-dried within a desiccator. The scanned surface area was standardized to 1 × 1 μm^2. Post-scanning, image analysis and processing were done using the Nanoscope Analysis 1.9 software (Brock Technology).

2.6.7. Small angle X-ray scattering (SAXS)

The structural analysis of micelles was done utilizing a SAXSpoint 2.0 device (Anton-Paar GmbH, Graz, Austria) operating with 1.54 Å radiation (Mata, Udabage, & Gilbert, 2011). The micelle dispersions and powders were placed onto a 2 mm thick sample stage with drilled rectangle holes (20 × 4 mm^2) and sealed on both sides using adhesive tapes. The scattered intensity was measured using a detector 600 mm from the sample and scattering was done in a vacuum for 1 h. The data obtained was subsequently processed using the SAXS analysis 4.00.046 software. The background scattering was obtained from an empty platform and subtracted from the sample's scattering data.

2.6.8. Confocal laser scanning microscopy (CLSM)

The microstructural characteristics of the gastric digesta were observed utilizing a CLSM (Leica TCS SP8, Leica Microsystems, Heidelberg, Germany) with an excitation wavelength of 488 nm and emission wavelengths ranging from 498 to 532 nm (Zou et al., 2022). The flocculates (100 μg) were labeled using fluorescein isothiocyanate isomer I (0.2%, w/v) for 20 min and then placed into a glass bottom cell culture dish. Imaging was done using a 10× objective lens.

2.6.9. Sodium dodecyl sulphate-polyacrylamide gel electrophoresis (SDS-PAGE)

SDS-PAGE on gastric *in vitro* digesta was done using a Mini-PROTEAN Tetra Cell system (Bio-Rad) loaded with a 4% stacking gel and a 12% resolving gel following Liu et al. (2019). The samples were mixed with the sample buffer (pH 6.8, containing Tris-HCl (62.5 mM), β-mercaptoethanol (5%), glycerol (10%, v/v) and bromophenol blue). The mixing ratio of the sample to the sample buffer was 1:1 (v/v). This mixture was boiled for 3 min and then loaded onto the gel. The voltages were 60 V for the stacking gel and 120 V for the resolving gel. Following electrophoresis, the gel was stained using 0.1% (w/v) Coomassie Brilliant Blue R-250 in methanol (50%, v/v) and acetic acid (6.8%, v/v) for 4 h. The gels were subsequently destained using 7.5% (v/v) acetic acid and 5% (v/v) methanol until distinct bands became visible and analyzed as previously (section 2.6.1).

2.6.10. OPA spectrophotometric assay

The determination of free amino groups followed Ménard et al. (2018) using 0–3 mM L-leucine as the standard. Digesta was mixed with TCA (3.12%, w/v) at a ratio of 1:1 (v/v) and then the mixture were centrifuged at 10,000×*g* for 0.5 h. The supernatant (150 μL) was combined with 3 mL OPA reagent consisting of 0.08% (w/v) OPA, 0.1% (w/v) SDS, 3.8% (w/v) $Na_2B_4O_7$ and 0.09% (w/v) dithiothreitol. A 150 μL aliquot of the standard or supernatant was combined with 3 mL of the OPA reagent and incubated for 15 min, and the absorbance measured at 340 nm.

2.6.11. High performance size exclusion chromatography (HPSEC)

The molecular weight distribution of peptides in the digesta was measured using the Waters e2695 Separations Module, which was equipped with a TSK gel G2000SWXL column (300 × 7.8 mm I.D., Tosoh Bioscience LLC, Montgomeryville, PA, USA), following Wang et al. (2023). The mobile phase was 0.1 M sodium phosphate buffer (pH 6.7) containing trifluoroacetic acid (0.1%, v/v) at a flow rate of 1 mL/min. Samples of 10 μL were injected and the eluted peptides were obtained at 220 nm.

2.7. Statistical analysis

Statistical analysis was done using the Statistical Analysis System version 8 (SAS Institute, Inc., Cary, NC, USA). One-way analysis of variance with the General Linear Model procedure was done. Significance was established at $P < 0.05$. All tests for each sample were replicated three times. The reported results were calculated means and their respective standard deviations.

3. Results and discussion

3.1. Formulation of caseins and modification of casein phosphorylation patterns

The protein composition of formulated caseins is shown in Fig. S1. The ratio of β-casein, κ-casein and α_{s1}-casein was 67.1:20.4:12.5 in the formulated caseins, with no detected α_{s2}-casein. This was close to the casein composition of human milk, where the ratio of β-casein, κ-casein and α_{s1}-casein was in the range of 68–70:18–21:9–12 (Hailu et al., 2016; Yang et al., 2022). The urea-PAGE pattern of human skim milk from 10 mothers showed 6 typical β-casein bands (Fig. S2). These bands corresponded to the mixed phosphorylation patterns of β-casein with 0–5 phosphate groups (0-P, 1-P, 2-P, 3-P, 4-P, 5-P) based on the increasing electrophoretic mobility. These results were consistent with Molinari, Casadio, Hartmann, Arthur, and Hartmann (2013). The phosphorylated isoforms of β-casein in human milk from 10 mothers showed a percentage range from 4.3 to 30.8% for 0-P, 11.6–19.6% for 1-P, 12.4–27.9% for 2-P, 8.6–16.3% for 3-P, 17.2–29.3 % for 4-P and 4.6–15.5 % for 5-P, respectively (Table S1).

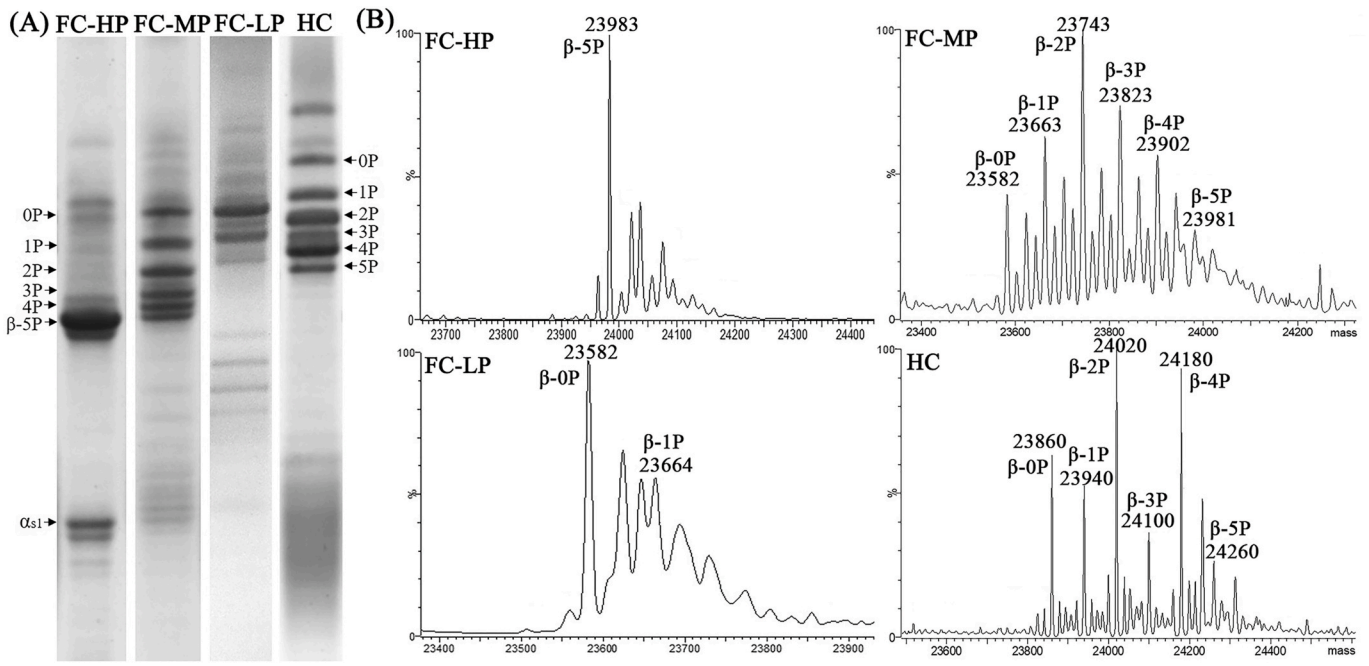

Fig. 1. Urea-PAGE patterns of total caseins (A) and deconvoluted mass spectra of β-casein (B) in formulated caseins with high, mixed and low phosphorylation patterns and human caseins. FC, formulated caseins; HP, high phosphorylation; MP, mixed phosphorylation; LP, low phosphorylation; HC, human caseins of mixed milk from 10 mothers; β, β-casein; α_{s1}, α_{s1}-casein; -nP, refers to the number of phosphate groups.

To simulate the mixed phosphorylation patterns of human caseins (HC), the formulated caseins were dephosphorylated for different times (Fig. S3). The number of bands, corresponding to β-casein isoforms just above the original β-casein band, increased within the initial 1 min of incubation. However, after 30 min of incubation, the number of bands gradually decreased until the end of the incubation. For each intermediate phosphorylated β-casein isoform, the electrophoretic mobility of the corresponding band further decreased with the removal of one more phosphate group, due to the decrease in net charge-to-mass ratio (Li-Chan et al., 1989). This indicated that none of the intermediate isoform was resistant to further dephosphorylation. Beyond the 180 min of incubation, multiple bands emerged above the dye front (Fig. S3), suggesting a proteolytic side reaction with prolonged incubation with phosphatase (Li-Chan et al., 1989). None of the dephosphorylated caseins were found to contain 6 phosphorylated β-casein isoforms at any time point, and the 0-P, 1-P, 2-P and 4-P isoforms were not simultaneously predominant (Fig. S3), suggesting a non-selectivity of the phosphatase towards phosphorylation sites. The mixed phosphorylation pattern of human β-casein was assumed to be simulated by mixing the high, medium and low phosphorylated isoforms of bovine β-casein, which were predominant at the initial, middle and end periods of dephosphorylation (Fig. S3), respectively. Therefore, according to the results of a series of preliminary experiments on mixing formulated caseins dephosphorylated for different times and at their different ratios, the formulated caseins dephosphorylated for 1, 15 and 180 min were mixed at a ratio of 1:2:0.4 to obtain formulated caseins with mixed phosphorylation patterns (FC-MP) for β-casein, which is similar to human caseins. In addition, the formulated caseins dephosphorylated for 0 and 180 min were used as the samples with high phosphorylated (FC-HP) and low phosphorylation patterns (FC-LP), respectively.

Urea-PAGE patterns of total caseins in formulated caseins with different phosphorylation patterns and human caseins are shown in Fig. 1A. The FC-HP showed one typical band, which corresponded to the 5-P isoform of β-casein. FC-MP showed 6 typical bands, corresponding to isoforms of β-casein with 0–5 phosphate groups, based on the increasing electrophoretic mobility, which was similar to the phosphorylated isoforms of human caseins. For FC-MP, the percentages of β-casein isoforms with 0-P, 1-P, 2-P, 3-P, 4-P and 5-P were 19.0, 19.6, 19.7 12.6, 16.7 and 12.3%, respectively (Table S1), which was within the percentages range of phosphorylated isoforms of β-casein in human caseins (Table S1). For FC-LP, two major phosphorylated β-casein isoforms were identified, with the percentages of 54.7% for 0-P and 37.5% for 1-P (Table S1).

To characterize the numbers of phosphate groups, deconvoluted mass spectra of β-casein in formulated caseins with different phosphorylation patterns and human caseins was shown in Fig. 1B. For FC-HP, the deconvolution of the multi-charged mass spectrum gave the appearance of major peak at 23,983 Da, which corresponded to β-casein with 5 phosphate groups. For FC-MP, based on the reduction in molecular weight compared to the original β-casein, 6 peaks at 23,981, 23,902, 23,823, 23,743, 23,663 and 23,582 Da were identified, corresponding to β-casein isoforms with decreasing phosphate groups (5-P to 0-P). For FC-LP, 2 major β-casein isoforms with 0 and 1 phosphate groups were identified, corresponding to 23,664 and 23,582 Da. For human caseins, 6 typical peaks at 23,860, 23,940, 24,020, 24,100, 24,180 and 24,260 Da were identified, showing 6 isoforms of human β-casein with 0–5 phosphate groups (Fig. 1B). Taken together, the phosphorylated isoforms of FC-MP and human caseins were similar, and these results were consistent with those of urea-PAGE shown in Fig. 1A.

3.2. Formation of casein micelles

The mean concentrations of Ca, Mg, Cit, and P_i in milk samples from 10 mothers were 7.1, 1.5, 2.3 and 2.8 mM, respectively. These results were consistent with the values of 7.3–7.8 mM for Ca, 1.4–1.6 mM for Mg, 2.2–2.8 mM for Cit and 2.2–2.5 mM for P_i as reported by Holt (1993) and Holt and Jenness (1984). The Ca concentrations in dispersions of FC-HP, FC-MP and FC-LP were 2.2, 1.9 and 1.6 mM, respectively, and the contents of Mg, Cit and P_i were <0.1 mM. The assembly of caseins in milk is significantly influenced by minerals, especially Ca (Neville, 2005). The formulated casein dispersions were supplemented with different concentrations of Ca with the mean concentrations of Mg, Cit and P_i in human skim milk to induce the formation of casein micelles.

Optical absorbance is associated with size, number and density of colloidal particles (Hemar et al., 2020). As shown in Fig. 2A, with

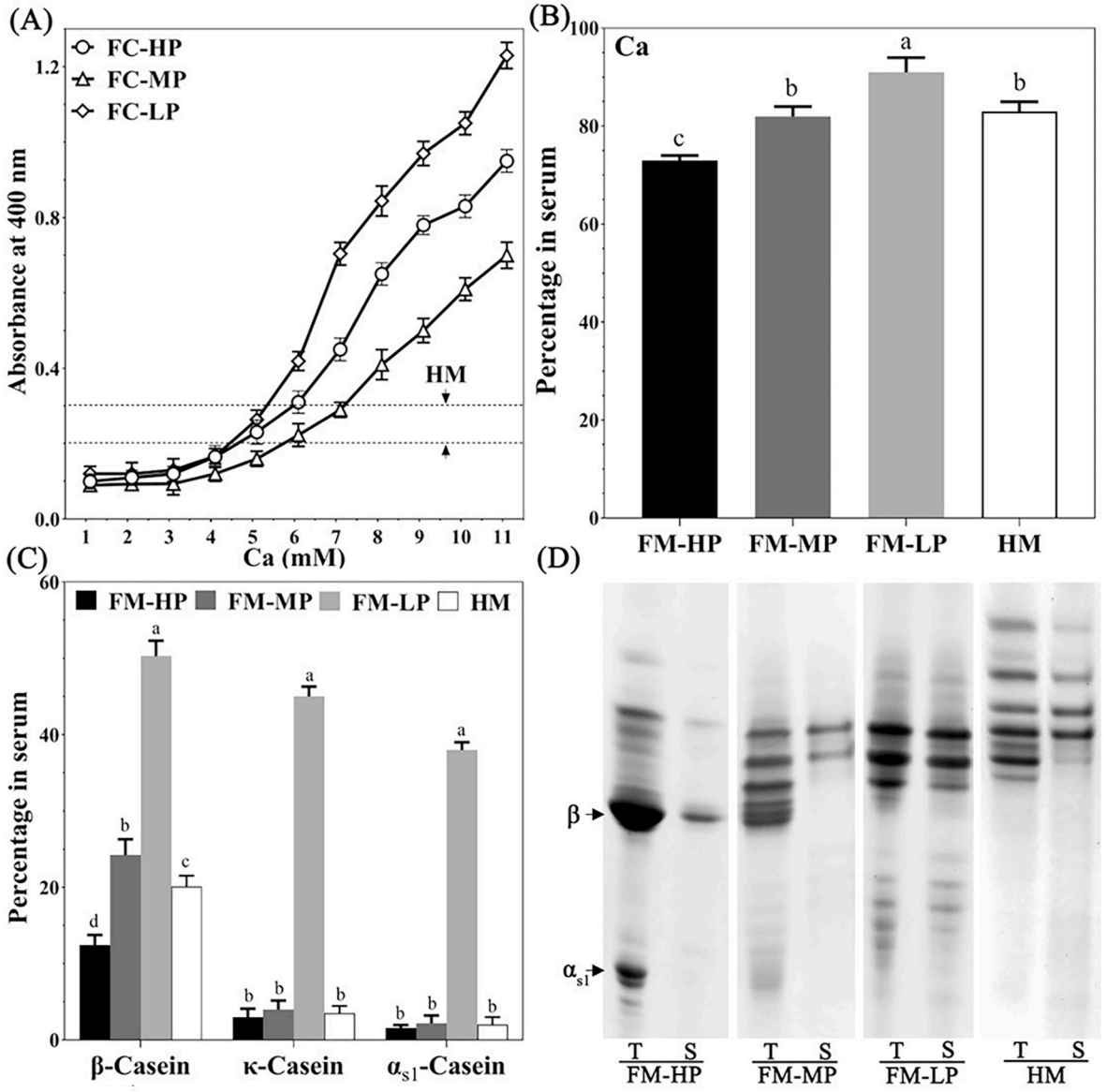

Fig. 2. Optical absorbance of dispersions of formulated caseins with high, mixed and low phosphorylation patterns with 1.1–11.1 mM Ca at a Ca:Mg molar ratio of 7.1:1.5 in the presence of 2.3 mM Cit and 2.8 mM P_i (A), percentage of serum Ca relative to total Ca (B), percentage of serum caseins (β, κ, α_{s1}) relative to total of corresponding casein (C) and urea-PAGE patterns of total and serum caseins (D) for casein micelles formed from formulated caseins with high, mixed and low phosphorylation patterns using 7.1 mM Ca and 1.5 mM Mg in the presence of 2.3 mM Cit and 2.8 mM P_i and human casein micelles. The two dotted lines show the range of optical absorbance of human casein micelle dispersions. a–d: different lower-case letters indicate that the data differ significantly among different samples ($P < 0.05$); FC, formulated casein micelles; FM, formed casein micelles; HP, high phosphorylation; MP, mixed phosphorylation; LP, low phosphorylation; HM, human casein micelles; β, β-casein; α_{s1}, α_{s1}-casein; T, total; S, serum.

increasing concentration of Ca, the absorbances of all casein dispersions remained almost unchanged between 1.1 and 4.1 mM Ca. Subsequently, absorbances increased gradually between 5.1 and 7.1 mM Ca, followed by a pronounced increase from 8.1 to 11.1 mM Ca, suggesting the progressive development of colloidal particles. Huppertz et al. (2017) also reported that colloidal particles, i.e., formed casein micelles with mineralization and a size similar to original bovine micelles were obtained through the utilization of sodium caseinate combined with Ca, Mg and P_i. At a same Ca concentration, the absorbance increased in order of FC-MP < FC-HP < FC-LP. At the mean Ca concentration found in human milk, the absorbance values determined for the FC-MP dispersion fell within the range for human micelles. These results agreed with previous reports that compared to original bovine caseins, the partially dephosphorylated caseins tended to form smaller colloidal particles with the presence of Ca, while the highly dephosphorylated caseins tended to form larger colloidal particles (Antuma et al., 2023; Schmidt & Poll, 1989; Song et al., 2023). Based on Fig. 2A, casein micelles, formed from Ca (7.1 mM) together with Mg (1.5 mM), Cit (2.3 mM) and P_i (2.8 mM), were used for subsequent studies.

3.3. Physicochemical properties of formed casein micelles

3.3.1. Distribution of Ca and caseins

Fig. 2B shows the percentages of serum Ca relative to total Ca for casein micelles formed from formulated caseins with high, mixed and low phosphorylation patterns and human micelles (HM). With the increase of degree of dephosphorylation, the percentages of serum Ca increased gradually, from 73% for FM-HP, to 82% for FM-MP and 91% for FM-LP (Fig. 2B). The serum Ca for FM-MP was similar to that for human micelles (83%). This was consistent with the value of ~70–80%

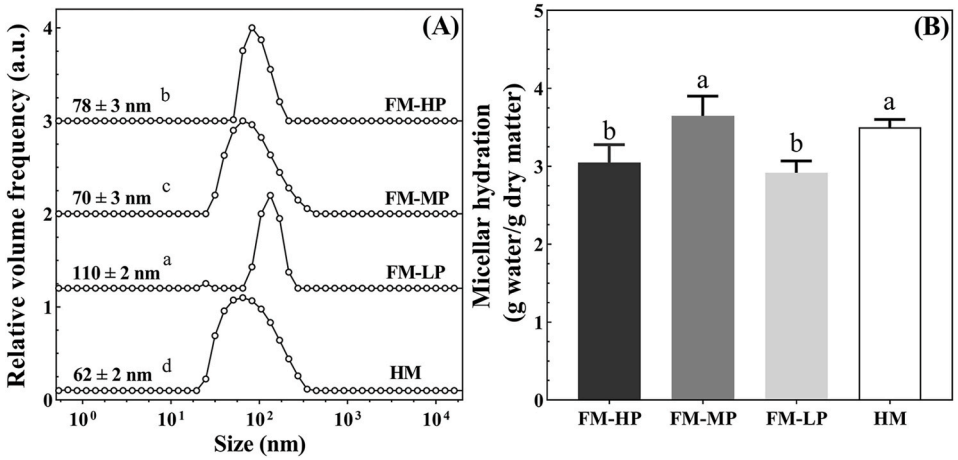

Fig. 3. Particle size distribution (A) and micellar hydration (B) of casein micelles formed from formulated caseins with high, mixed and low phosphorylation patterns and human casein micelles. FM, formed casein micelles; HP, high phosphorylation; MP, mixed phosphorylation; LP, low phosphorylation; HM, human casein micelles; a–d: different lower-case letters indicate that the data differ significantly among different samples ($P < 0.05$).

serum Ca in human milk reported by Holt (1993) and Holt and Jenness (1984). With the increase in the degree of dephosphorylation, the percentages of serum β-casein, κ-casein and α_{s1}-casein in relation to their respective total concentrations (Fig. 2C) increased gradually from 12, 3, and 2% for FM-HP, to 24, 4, and 2% for FM-MP, and to 50, 45, and 38% for FM-LP (Fig. 2C). The serum β-casein was markedly higher than that of serum α_{s1}-and κ-casein. Zhang et al. (2024) reported a preferential dissociation of β-casein from caprine micelles after dephosphorylation, which also suggested a different role of β-casein in micellar assembly (Dalgleish & Corredig, 2012). For FM-MP, the percentages of serum β-casein, κ-casein and α_{s1}-casein were similar to that of human micelles, i.e., with β-casein, κ-casein and α_{s1}-casein at a percentage of 20, 4, and 2% (Fig. 2C). For FM-HP and FM-MP, the caseins in serum were mainly the isoforms with lower electrophoretic mobility (Fig. 2D), i.e., a lower number of phosphate groups. Casein isoforms with fewer phosphate groups tend to establish fewer ionic bonds with colloidal Ca, resulting in diminished associative interactions within the internal structure of the micelles, thus leading to Ca and caseins moving into the serum (Antuma et al., 2023; Yamauchi, Takemoto, & Tsugo, 1967). Zhang et al. (2024) reported that the serum Ca and serum caseins dissociated from caprine micelles after dephosphorylation increased with the increase of degree of dephosphorylation, which also suggested the crucial role of casein phosphate groups in assembly of caseins and minerals into micelles. These results were consistent with the results reported by Yang et al. (2022) that in human milk, β-casein existed as mixed phosphorylated isoforms having 0–5 phosphate groups, which in serum was mainly the isoforms with 0–2 phosphate groups.

3.3.2. *Particle size distributions and micellar hydration*

Fig. 3 shows the size distributions and micellar hydrations of the formed casein micelles and human casein micelles. The diameter (Fig. 3A) of FM-MP was smaller than that of FM-HP ($P < 0.05$), and closer to human micelles. The average diameter of FM-LP was much higher than that of FM-HP, FM-MP and human micelles. The micellar hydration (Fig. 3B) of FM-MP was higher than that of FM-HP and FM-LP, and similar to that of human micelles (Fig. 3B). The decreased particle size and the increased micellar hydration were consistent with the result of decreasing absorbance (Fig. 2A) as both the smaller particles and the looser particles had diminished scattering (Liu & Guo, 2008). Zhang et al. (2024) also reported that the size decreased and micellar hydration increased progressively with the degree of dephosphorylation increasing to 31% compared to original caprine micelles. After releasing micellar

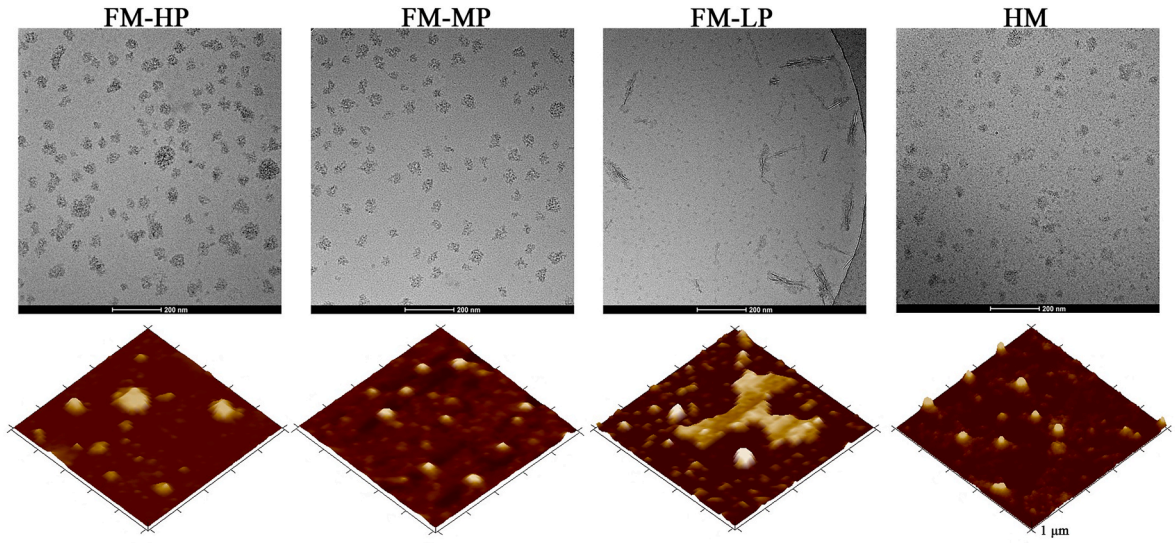

Fig. 4. Cryo-TEM (top) and AFM (bottom) micrographs of casein micelles formed from formulated caseins with high, mixed and low phosphorylation patterns and human casein micelles. FM, formed casein micelles; HP, high phosphorylation; MP, mixed phosphorylation; LP, low phosphorylation; HM, human casein micelles.

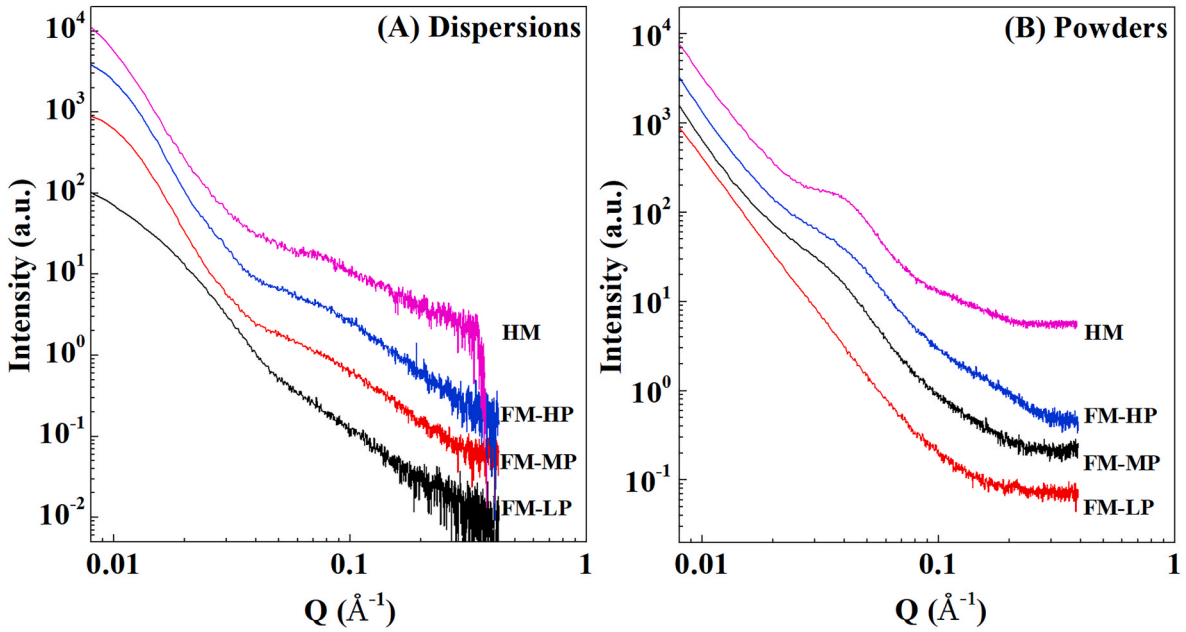

Fig. 5. SAXS profiles (A, dispersions; B, powders) for casein micelles formed from formulated caseins with high, mixed and low phosphorylation patterns and human casein micelles. FM, formed casein micelles; HP, high phosphorylation; MP, mixed phosphorylation; LP, low phosphorylation; HM, human casein micelles.

caseins and colloidal Ca, the residual micellar frameworks underwent an intra-micellar mass redistribution, leading to a relaxation or loosening of their overall structure, thereby trapping additional water inside the micelles. Antuma et al. (2023) reported that for micelles formed from bovine caseins and its dephosphorylated counterpart, the size increased and the micellar hydration decreased gradually as the percentage of dephosphorylated caseins increased from 40 to 100%. The release of a greater amount of negatively charged phosphate groups from κ- and β-caseins might be linked to an increase in hydrophobicity with a concomitant loss of negative charges, which could promote associative interactions among caseins, resulting in the increased particle size and the decreased micellar hydration (Mercier, Addeo, & Pelissier, 1976; Pepper & Thompson, 1963).

3.3.3. *Morphology and internal structure*

Fig. 4 shows the Cryo-TEM micrographs of the formed micelles and human micelles. FM-HP, FM-MP and human micelles all showed a generally spherical contour with a dark interior, which resembled the morphology of human casein micelles observed by Yang et al. (2022) using Cryo-TEM. Casein micelles in FM-HP, FM-MP and human micelles were uniformly dispersed and the size of FM-MP was closest to human micelles compared to FM-HP (Fig. 4). Whereas FM-LP showed irregular contours with apparently larger sizes, suggesting the crucial roles of the casein phosphate groups in micellar assembly. The above results were consistent with the particle size distribution shown in Fig. 3A. Similarly, individual micelles could be observed using AFM. FM-HP, FM-MP and human micelles all showed typical surface irregularities, which were similar to native bovine micelles observed by Ouanezar et al. (2012) using AFM, whereas FM-LP did not show the typical micellar morphology. These results were consistent with the results of Cryo-TEM, i.e., that the morphology and size of FM-MP were closest to that of human micelles.

For SAXS curves of human micelle dispersions (Fig. 5A), the low-Q region up to 0.03 Å^{-1} has been associated with the interfacial scattering originating from the spherical micelles, and the high-Q broad inflexion at 0.07 Å^{-1} has been linked to the local protein inhomogeneity within the micelles (Mata et al., 2011). For FM-HP and FM-MP, the scattering intensity over the low-Q region showed almost the same features as that of human micelles; while the corresponding scattering

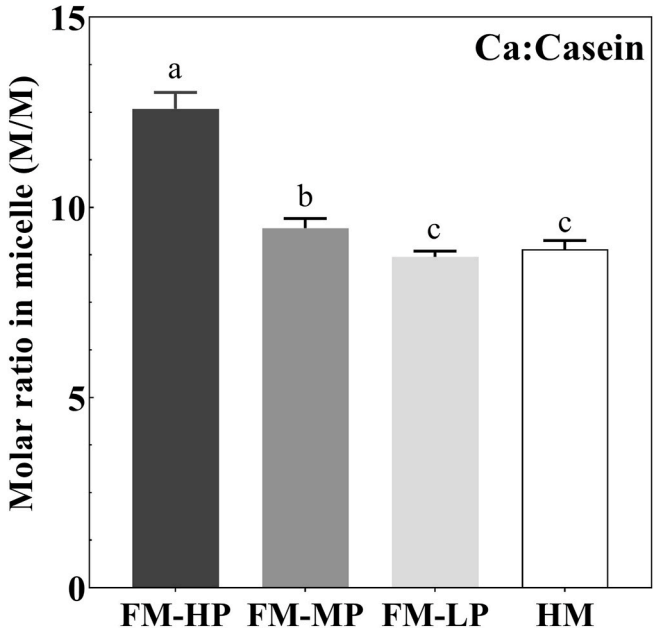

Fig. 6. Molar ratio of Ca:casein for casein micelles formed from formulated caseins with high, mixed and low phosphorylation patterns and human casein micelles; a–c: different lower-case letters indicate that the data differ significantly among different samples ($P < 0.05$); FM, formed casein micelles; HP, high phosphorylation; MP, mixed phosphorylation; LP, low phosphorylation; HM, human casein micelles.

intensity was markedly lower for FM-LP. These results were consistent with the Cryo-TEM observation that the spherical morphology of FM-HP and FM-MP was similar to human micelles, whereas FM-LP did not show typical micellar morphology (Fig. 4). Zhang et al. (2024) also noted that for caprine micelles, scattering in the low-Q region remained almost unchanged when the degree of dephosphorylation increased to 49%. The SAXS curves of FM-HP and FM-MP also showed the high-Q inflexion at 0.07 Å^{-1}, suggesting an intra-micellar local protein inhomogeneity similar to that in human micelles. For FM-LP, the high-Q inflexion was

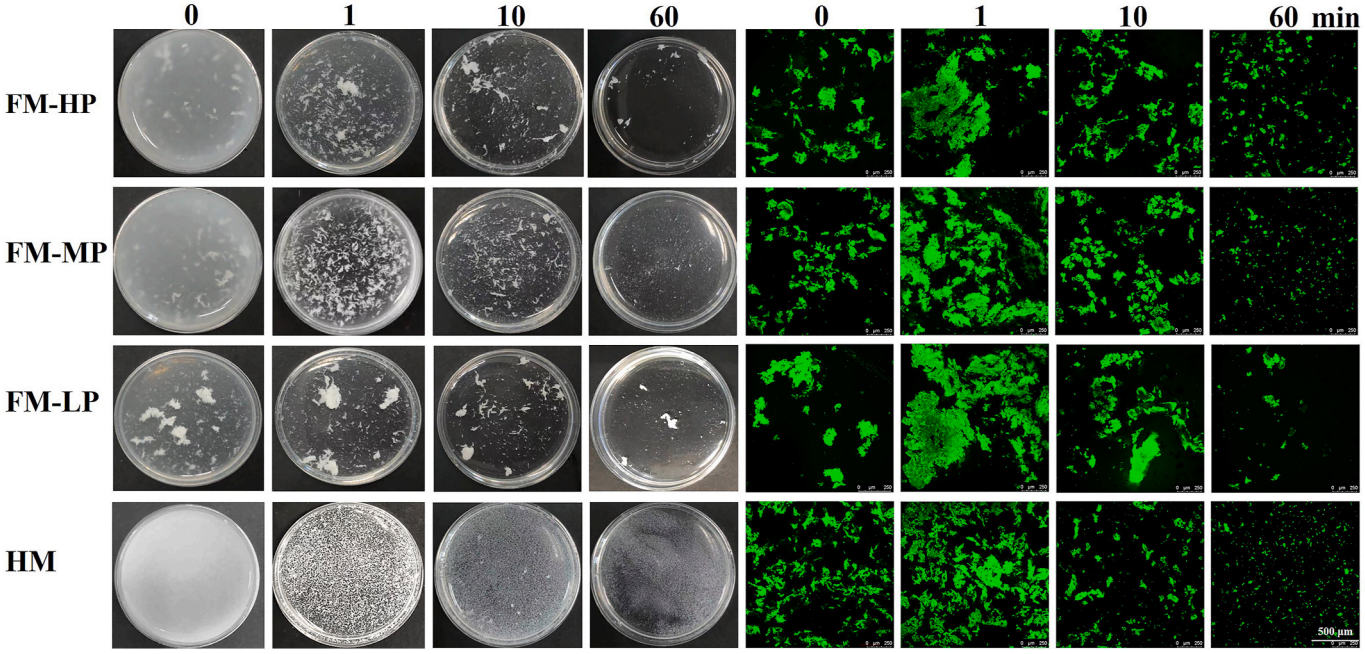

Fig. 7. Visual appearance (left) and CLSM micrographs (right) of the *in vitro* model of infant gastric digesta of casein micelles formed from formulated caseins with high, mixed and low phosphorylation patterns and human casein micelles. FM, formed casein micelles; HP, high phosphorylation; MP, mixed phosphorylation; LP, low phosphorylation; HM, human casein micelles.

not observed, suggesting a more homogenous internal mass distribution. These results indicated the important role of casein phosphate groups in forming the internal structures of casein micelles.

For SAXS curves of the human micelle powders (Fig. 5B), the broad inflection observed at 0.45 $Å^{-1}$ in the mid-Q range can be attributed to the average interparticle correlation length of Ca phosphate nanoclusters (CCP) within the micellar structure. The appearance of this inflexion likely arose from the heightened scattering contrast resulting from the displacement of water with air in the void spaces, along with the heightened packing density of CCP nanoclusters within the matrix after drying (Mata et al., 2011). The SAXS curves of FM-HP and FM-MP powders also showed the mid-Q inflexions at 0.45 $Å^{-1}$, indicating an intra-micellar formation and distribution of CCP nanoclusters similar to that in human micelles (Fig. 5B). For FM-LP, no characteristic inflexion was observed in the mid-Q, confirming that casein phosphate groups have an important role in forming the internal structures of micelles (Fig. 5A). This was in line with Schmidt and Poll (1989), who reported the formation of calcium phosphate particles stabilized by caseins, rather than of casein micelles, when mixing highly dephosphorylated bovine caseins with major minerals in milk. The Ca:casein molar ratio of

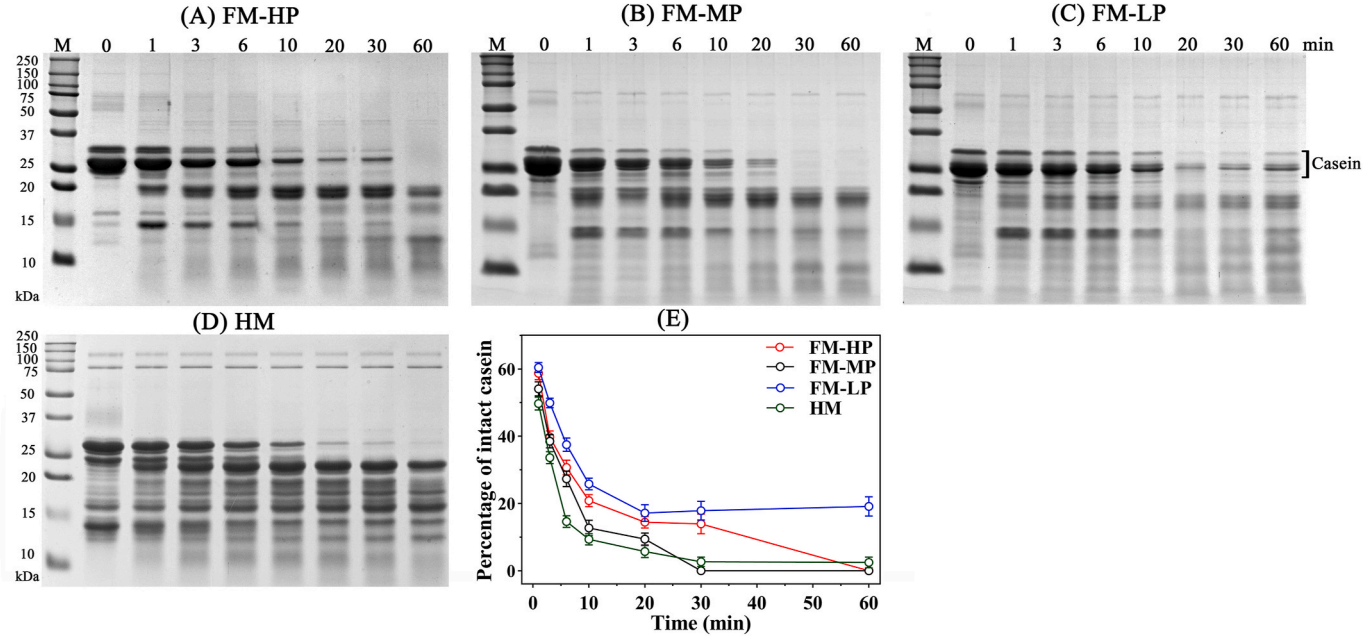

Fig. 8. SDS-PAGE patterns (A–D) and percentage of remaining intact caseins (E) of the *in vitro* model of infant gastric digesta of casein micelles formed from formulated caseins with high, mixed and low phosphorylation patterns and human casein micelles. FM, formed casein micelles; HP, high phosphorylation; MP, mixed phosphorylation; LP, low phosphorylation; HM, human casein micelles; M, protein markers.

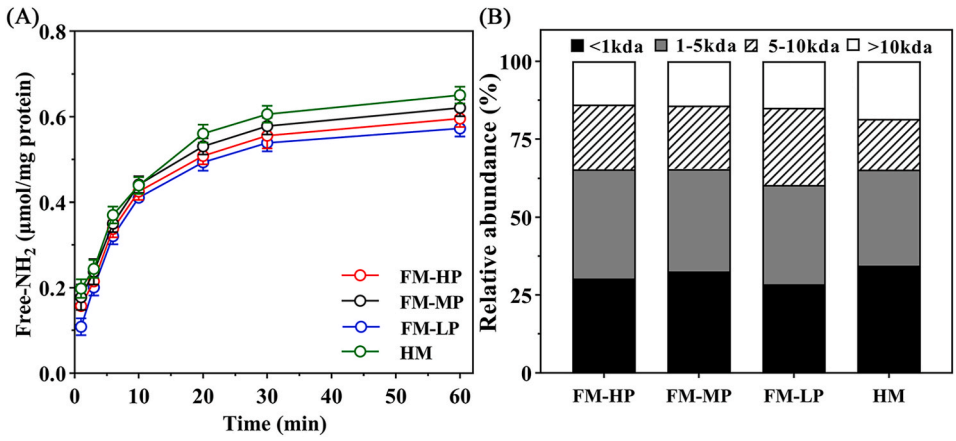

Fig. 9. Concentration of free amino groups (A) and molecular weight distribution of peptides (B) in the *in vitro* model of infant gastric digesta of casein micelles formed from formulated caseins with high, mixed and low phosphorylation patterns and human casein micelles. FM, formed casein micelles; HP, high phosphorylation; MP, mixed phosphorylation; LP, low phosphorylation; HM, human casein micelles.

micelles were shown in Fig. 6, with values of ~12.6 for FM-HP, ~9.4 for FM-MP and ~8.7 for FM-LP. The Ca:casein molar ratio of FM-MP was closer to that of human micelles (8.9) compared to FM-HP. Considering the results of SAXS curves and the molar ratio of Ca:casein, it can be suggested that the internal micellar structure of FM-MP was closer to that of the human micelles compared to FM-HP. Zhang et al. (2024) also reported that for caprine micelles, the mid-Q inflection showed a gradual decline ranging from 0 to 31% dephosphorylation, and subsequently vanished at 49% dephosphorylation. This was attributed to the progressive loss of colloidal Ca from the micelles as dephosphorylation increased.

3.4. Gastrointestinal digestibility with infants

3.4.1. Gastric flocs and protein hydrolysis

The morphological characteristics of the flocs generated during the gastric digestion of 4 samples are shown in Fig. 7. Upon acidification in the gastric fluid at the onset of digestion (0 min), all the samples formed small and loose flocs. Upon the addition of pepsin (1 min), substantial fragmented flocs formed, gradually diminishing in both size and density over the subsequent 60 min of digestion. At a same digestion time, the size of flocculated particles generally increased in an order of human micelles < FM-MP < FM-HP < FM-LP, and the flocs of FM-MP were similar to that of human micelles (Fig. 7).

The casein degradation during gastric digestion of the 4 samples is shown in Fig. 8. The intact casein bands gradually disappeared after 60, 30, and 10 min of digestion for FM-HP, FM-MP and human micelles, respectively (Fig. 8). For FM-LP, the percentage of intact caseins remained at ~18% at the end of digestion. The degradation rate of FM-MP was closest to that of human micelles. Simultaneously, several low molecular weight polypeptides were observed below the intact casein bands, and the major fractions were in the range of 15–20 and 15–25 kDa for formed micelles and human micelles, respectively, suggesting a difference in digestion patterns.

The evolution of free amino groups of various samples is shown in Fig. 9A. For all samples, a rapid increase in free amino group levels was observed during the initial 0.5 h, followed by a gradual rise until completion, suggesting an increasing level of proteolysis. Among the 3 formed micelles, the ascending order of free amino groups was observed as FM-LP < FM-HP < FM-MP, with the quantity of free amino groups in FM-MP closest to that of human micelles. The molecular weight distribution of peptides generated following 1 h of gastric digestion is shown in Fig. 9B. In all the samples, the concentration of the <1 kDa fractions generally followed the order of FM-LP < FM-HP < FM-MP < human micelles (Fig. 9B). Human micelles showed the highest concentration of <1 kDa fractions, and the concentration of >10 kDa fractions for human micelles was greater than those for the formed micelles, agreeing with the electrophoresis patterns of digested human micelles (Fig. 8D).

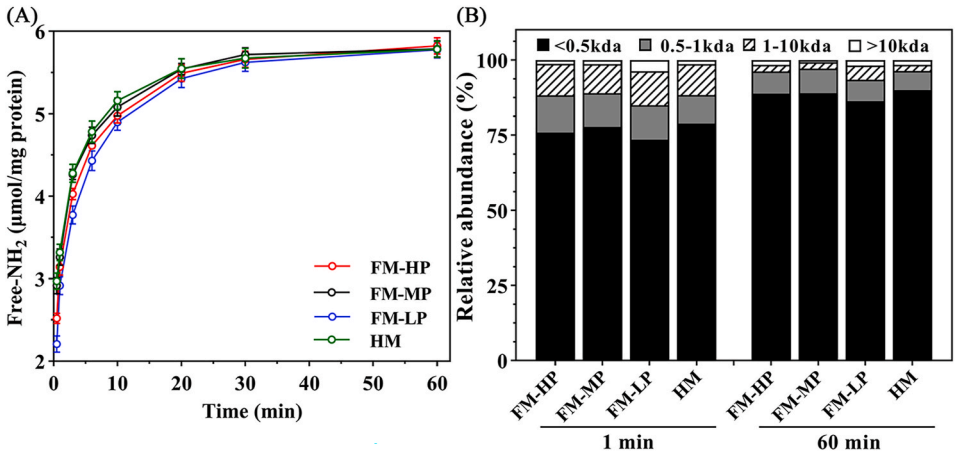

Fig. 10. Concentration of free amino groups (A) and molecular weight distribution of peptides (B) in the *in vitro* infant model of intestinal digesta of casein micelles formed from formulated caseins with high, mixed and low phosphorylation patterns and human casein micelles. FM, formed casein micelles; HP, high phosphorylation; MP, mixed phosphorylation; LP, low phosphorylation; HM, human casein micelles.

During gastric digestion, the decreased pH triggered the solubilization of colloidal Ca and the collapse of surface κ-casein hairy layers. Subsequently, pepsin-driven proteolysis led to the removal of κ-casein hairy layers, reducing both electrostatic and steric repulsion between micelles (Yahimi-Yazdi, Corredig, & Dalgleish, 2014). The removal of κ-casein hairy layers also exposed the Ca sensitive caseins nestled within the micelles, thus facilitating inter-micellar Ca-bridging (Huppertz & Chia, 2021). These concurrent effects collectively contributed to the formation of flocs throughout the gastric digestion process of the micelles. The inter-micellar Ca-bridging might decrease upon removing phosphate groups, contributing to the formation of smaller and looser flocs during gastric digestion (Liao et al., 2022). Moreover, the increased serum caseins with fewer phosphate groups (Fig. 2C and D) might hinder aggregation of the para-casein micelles by absorbing onto their surfaces during gastric digestion, thus forming looser flocs (Gaygadzhiev et al, 2012; Huppertz & Lambers, 2020).

The loose flocs formed by the mixed phosphorylated caseins might enhance the access of the digestive enzymes to the peptide bonds linkages within casein molecules. This, in turn, might increase both the speed of gastric emptying and the effectiveness of gastrointestinal proteolysis. Liu et al. (2019) reported that partial dephosphorylation of β-casein resulted in the formation of looser gastric clots with heightened gastrointestinal digestibility. The removal of more phosphate groups resulted in an increase of the isoelectric point of caseins, i.e., approaching the characteristic pH of 5.3 used in an infant stomach digestion model (Liu et al., 2016). This might lead to a great reduction in the net negative charge of caseins, concurrently weakening electrostatic repulsions and increasing hydrophobic associations, which in turn would facilitate the aggregation of casein molecules and the formation of larger flocs. Roy et al. (2020) reported that the larger and denser flocs formed may impede access of digestive enzymes to peptide bonds in casein molecules, resulting in reduced rates of gastric emptying and efficiency of gastrointestinal proteolysis. Therefore, using micelles formed from mixed rather than high or low phosphorylated caseins might result in looser gastric flocs and faster protein hydrolysis, similar to the infant digestion behaviors with human micelles.

3.4.2. *Intestinal proteolysis*

The concentration of free amino groups of different samples are shown in Fig. 10A. In all samples, a sharp rise in free amino groups occurred within the initial 30 min, followed by a gradual increase. During the initial 30 min, the order of free amino groups increased generally as FM-LP < FM-HP < FM-MP < human micelles, while no significant discrepancies were noted across different micelles at the completion of the digestion process. The distribution of peptides molecular weights is shown in Fig. 10B. For all samples, compared to the end of gastric digestion, a progressive decline in the concentration of >1 kDa fractions was observed, coupled with a simultaneous rise in the <1 kDa fractions throughout digestion. The concentration of the <0.5 kDa fraction generally followed the order of FM-LP < FM-HP < FM-MP < human micelles at 1 min of digestion. The concentration of the <0.5 kDa fraction for FM-HP, FM-MP and human micelles was slightly higher than for FM-LP at 60 min of digestion, with no significant differences observed among FM-HP, FM-MP and human micelles (Fig. 10B).

During intestinal digestion, the increase in pH levels led to an increase in inter-molecular electrostatic repulsions, thereby promoting the dissolution of the digesta. This facilitated greater access of trypsin and chymotrypsin to peptide bonds, accelerating protein hydrolysis (Halabi et al., 2022). With infant conditions, characterized by a lower pancreatic enzyme level, distinctions in proteolysis persisted among FM-LP, FM-HP, FM-MP and human micelles over the initial 30 min of digestion (Fig. 9A and B), further showing that the digestibility of FM-MP was better than that of FM-LP, FM-HP and closer to that of human micelles. Moreover, as reported by Wang et al. (2023), variations in proteolysis levels among bovine micelles showing varying levels of demineralization continued during the initial 30 min of intestinal digestion with infant conditions, with minimal differences observed at the end of the digestion.

4. Conclusion

The caseins from the bovine caseins were fractionated and formulated according to the composition of human casein, followed by dephosphorylation for different times. The formulated caseins dephosphorylated for 1, 15 and 180 min were mixed at a ratio of 1:2:0.4 to obtain FC-MP with 0–5 P, similar to human β-casein. With the average mineral concentrations of human milk, the formed casein micelles (FM-HP, FM-MP, FM-LP) were obtained by adding minerals into the formulated casein dispersions with different phosphorylation patterns. The optical absorbances, particle size, micellar hydration, Ca:casein molar ratio and micellar morphology of FM-MP were closer to that of human micelles compared to FM-HP and FM-LP. The gastric flocs, casein degradation rate, and free amino groups of digested FM-MP were also closer to that of human micelles compared to FM-HP and FM-LP. These results suggested the importance of phosphorylation in facilitating the assembly of casein into micellar structures, with implications for their application in infant formulae. FM-MP as part of infant formulae should be further studied as a beneficial replacement for human micelles, such as the patterns of bioactive peptides released after gastrointestinal digestion. The formed casein micelles could be potentially used as protein and mineral supplements for other populations with low secretion levels of gastric acid and digestive proteases.

CRediT authorship contribution statement

Tingting Yang: Writing – review & editing, Writing – original draft, Methodology, Investigation, Data curation. **Xinhuizi Hong:** Software, Methodology. **Xiumei Tao:** Writing – review & editing, Supervision. **Jielong Zhang:** Writing – review & editing, Software, Methodology. **Dasong Liu:** Writing – review & editing, Project administration, Methodology, Investigation. **Xiaoming Liu:** Writing – review & editing. **Thom Huppertz:** Writing – review & editing. **Joe M. Regenstein:** Writing – review & editing. **Peng Zhou:** Writing – review & editing, Funding acquisition.

Declaration of competing interest

The authors declare that they have no known competing financial interests or personal relationships that could have appeared to influence the work reported in this paper.

Data availability

Data will be made available on request.

Acknowledgements

This study was partly supported by the National Key R&D Program of China (2023YFF1103403), the National Natural Science Foundation of China (31901613), the National High-end Foreign Expert Project of China (G2022144006L), the Wuxi Science and Technology Development Fund Project (K20231027), the Fundamental Research Funds for the Central Universities (JUSRP121077), and the Collaborative Innovation Centre of Food Safety and Quality Control of Jiangsu Province.

Appendix A. Supplementary data

Supplementary data to this article can be found online at https://doi.org/10.1016/j.foodhyd.2024.110020.

References

Andrews, A. T. (1983). Proteinases in normal bovine milk and their action on caseins. *Journal of Dairy Research, 50*, 45–55.

Antuma, L. J., Braitmaier, S. H., Garamus, V. M., Hinrichs, J., Boom, R. M., & Keppler, J. K. (2024). Engineering artificial casein micelles for future food: Preparation rate and coagulation properties. *Journal of Food Engineering, 366*. Article 111868.

Antuma, L. J., Steiner, I., Garamus, V. M., Boom, R. M., & Keppler, J. K. (2023). Engineering artificial casein micelles for future food: Is casein phosphorylation necessary? *Food Research International, 173*. Article 113315.

Bansal, N., Fox, P. F., & Mcsweeney, P. L. H. (2007). Aggregation of rennet-altered casein micelles at low temperatures. *Journal of Agricultural and Food Chemistry, 55*, 3120–3126.

Berton, A., Rouvellac, S., Robert, B., Rousseau, F., Lopez, C., & Crenon, I. (2012). Effect of the size and interface composition of milk fat globules on their *in vitro* digestion by the human pancreatic lipase: Native versus homogenized milk fat globules. *Food Hydrocolloids, 29*, 123–134.

Bourlieu, C., Ménard, O., Bouzerzour, K., Mandalari, G., Macierzanka, A., Mackie, A. R., et al. (2014). Specificity of infant digestive conditions: Some clues for developing relevant *in vitro* models. *Critical Reviews in Food Science and Nutrition, 54*, 1427–1457.

Brodkorb, A., Egger, L., Alminger, M., Alvito, P., Assunção, R., Ballance, S., et al. (2019). INFOGEST static *in vitro* simulation of gastrointestinal food digestion. *Nature Protocols, 14*, 991–1014.

Dalgleish, D. G., & Corredig, M. (2012). The structure of the casein micelle of milk and its changes during processing. *Annual Review of Food Science and Technology, 3*, 449–467.

Garnsworthy, P. C., Masson, L. L., Lock, A. L., & Mottram, T. T. (2006). Variation of milk citrate with stage of lactation and *de novo* fatty acid synthesis in dairy cows. *Journal of Dairy Science, 89*, 1604–1612.

Gaygadzhiev, Z., Massel, V., Alexander, M., & Corredig, M. (2012). Addition of sodium caseinate to skim milk inhibits rennet-induced aggregation of casein micelles. *Food Hydrocolloids, 26*, 405–411.

Hailu, Y., Hansen, E. B., Seifu, E., Eshetu, M., Ipsen, R., & Kappeler, S. (2016). Functional and technological properties of camel milk proteins: A review. *Journal of Dairy Research, 83*, 422–429.

Halabi, A., Croguennec, T., Ménard, O., Briard-Bion, V., Jardin, J., Gouar, Y. L., et al. (2022). Protein structure in model infant milk formulas impacts their kinetics of hydrolysis under *in vitro* dynamic digestion. *Food Hydrocolloids, 126*. Article 107368.

Hemar, Y., Xu, C., Wu, S., & Ashokkumar, M. (2020). Size reduction of "reformed casein micelles" by high-power ultrasound and high hydrostatic pressure. *Ultrasonics Sonochemistry, 63*. Article 104929.

Holt, C. (1993). Interrelationships of the concentrations of some ionic constituents of human milk and comparison with cow and goat milks. *Comparative Biochemistry and Physiology, 104*, 35–41.

Holt, C., & Jenness, R. (1984). Interrelationships of constituents and partition of salts in milk samples from eight species. *Comparative Biochemistry and Physiology Part A: Physiology, 77*, 275–282.

Huppertz, T., & Chia, L. W. (2021). Milk protein coagulation under gastric conditions: A review. *International Dairy Journal, 113*. Article 104882.

Huppertz, T., Gazi, I., Luyten, H., Nieuwenhuijse, H., Alting, A., & Schokker, E. (2017). Hydration of casein micelles and caseinates: Implications for casein micelle structure. *International Dairy Journal, 74*, 1–11.

Huppertz, T., & Lambers, T. T. (2020). Influence of micellar calcium phosphate on *in vitro* gastric coagulation and digestion of milk proteins in infant formula model systems. *International Dairy Journal, 107*. Article 104717.

ISO. (2001). *Milk - determination of nitrogen content - Part 5: Determination of protein-nitrogen content*. Geneva, Switzerland: International Standardisation Organisation. *ISO 8968-5*.

ISO. (2018). *Milk, milk products, infant formula and adult nutritionals - determination of minerals and trace elements - Inductively coupled plasma mass spectrometry (ICP-MS) method*. Geneva, Switzerland: International Standardisation Organisation. ISO 21424-11.

Li-Chan, E., & Nakai, S. (1989). Enzymic dephosphorylation of bovine casein to improve acid clotting properties and digestibility for infant formula. *Journal of Dairy Research, 56*, 381–390.

Liao, M. J., Chen, F., Hu, X. S., Miao, S., Ma, L. J., & Ji, J. F. (2022). The *in-vitro* digestion behaviors of micellar casein acting as wall materials in spray-dried microparticles: The relationships between colloidal calcium phosphate and the release of loaded blueberry anthocyanins. *Food Chemistry, 375*. Article 131864.

Liu, Y., & Guo, R. (2008). pH-dependent structures and properties of casein micelles. *Biophysical Chemistry, 136*, 67–73.

Liu, D. S., Wang, Y. Y., Yu, Y., Hu, J. H., Lu, N. Y., Regenstein, J. M., et al. (2016). Effects of enzymatic dephosphorylation on infant *in vitro* gastrointestinal digestibility of milk protein concentrate. *Food Chemistry, 197*, 891–899.

Liu, D. S., Zhang, J., Wang, L. L., Yang, T. Y., Liu, X. M., Hemar, Y., et al. (2019). Membrane-based fractionation, enzymatic dephosphorylation, and gastrointestinal digestibility of β-casein enriched serum protein ingredients. *Food Hydrocolloids, 88*, 1–12.

Mata, J. P., Udabage, P., & Gilbert, E. P. (2011). Structure of casein micelles in milk protein concentrate powders via small angle X-ray scattering. *Soft Matter, 7*, 3837–3843.

Ménard, O., Bourlieu, C., De Oliveira, S. C., Dellarosa, N., Laghi, L., Carriere, F., et al. (2018). A first step towards a consensus static *in vitro* model for simulating full-term infant digestion. *Food Chemistry, 240*, 338–345.

Meng, F., Uniacke-Lowe, T., Ryan, A. C., & Kelly, A. L. (2021). The composition and physico-chemical properties of human milk: A review. *Trends in Food Science & Technology, 112*, 608–621.

Mercier, J. C., Addeo, F., & Pelissier, J. P. (1976). Primary structure of the casein macropeptide of caprine kappa casein. *Biochimie, 58*, 1303–1310.

Minekus, M., Alminger, M., Alvito, P., Ballance, S., Bohn, T., Bourlieu, C., et al. (2014). A standardised static *in vitro* digestion method suitable for food-An international consensus. *Food & Function, 5*, 1113–1124.

Molinari, C. E., Casadio, Y. S., Hartmann, B. T., Arthur, P. G., & Hartmann, P. E. (2013). Longitudinal analysis of protein glycosylation and β-casein phosphorylation in term and preterm human milk during the first 2 months of lactation. *British Journal of Nutrition, 110*, 105–115.

Ouanezar, M., Guyomarc'h, F., & Bouchoux, A. (2012). AFM imaging of milk casein micelles: Evidence for structural rearrangement upon acidification. *Langmuir, 28*, 4915–4919.

Pepper, L., & Thompson, M. P. (1963). Dephosphorylation of α_s-and κ-caseins and its effect on micelle stability in the κ-α_s-casein system. *Journal of Dairy Science, 46*, 764–767.

Pitkowski, A., Nicolai, T., & Durand, D. (2008). Scattering and turbidity study of the dissociation of casein by calcium chelation. *Biomacromolecules, 9*, 369–375.

Post, A. E., Arnold, B., Weiss, J., & Hinrichs, J. (2012). Effect of temperature and pH on the solubility of caseins: Environmental influences on the dissociation of α_s-and β-casein. *Journal of Dairy Science, 95*, 1603–1616.

Poth, A. G., Deeth, H. C., Alewood, P. F., & Holland, J. (2008). Analysis of the human casein phosphoproteome by 2-D electrophoresis and MALDI-TOF/TOF MS reveals new phosphoforms. *Journal of Proteome Research, 7*, 5017–5027.

Power, O. M., Fenelon, M. A., O'Mahony, J. A., & McCarthy, N. A. (2019). Dephosphorylation of caseins in milk protein concentrate alters their interactions with sodium hexametaphosphate. *Food Chemistry, 271*, 136–141.

Roy, D., Ye, A., Moughan, P. J., & Singh, H. (2020). Composition, structure, and digestive dynamics of milk from different species - a review. *Frontiers in Nutrition, 7*. Article 577759.

Schmidt, D. G., & Poll, J. K. (1989). Properties of artificial casein micelles. 4. Influence of dephosphorylation and phosphorylation of the casein. *Netherlands Milk and Dairy Journal, 43*, 53–62.

Semagoto, H. M., Liu, D. S., Koboyatau, K., Hu, J. H., Lu, N. Y., Liu, X. M., et al. (2014). Effects of UV induced photo-oxidation on the physicochemical properties of milk protein concentrate. *Food Research International, 62*, 580–588.

Song, S. J., Lin, Y. Y., Zhang, Y. N., Luo, Y. J., & Guo, H. Y. (2023). The self-association properties of partially dephosphorylated bovine beta-casein. *Food Hydrocolloids, 134*. Article 108019.

Sood, S. M., Erickson, G., & Slattery, C. W. (2005). The formation of casein micelles reconstituted with Ca^{2+} and added inorganic phosphate is influenced by the non-phosphorylated form of human β-casein. *The Protein Journal, 24*, 227–232.

Sood, S. M., Lekic, T., Jhawar, H., Farrell, H. M., & Slattery, C. W. (2006). Reconstituted micelle formation using reduced, carboxymethylated bovine κ-casein and human β-casein. *The Protein Journal, 25*, 352–360.

Thienel, K. J., Holder, A., Schubert, T., Boom, R. M., Hinrichs, J., & Atamer, Z. (2018). Fractionation of milk proteins on pilot scale with particular focus on β-casein. *International Dairy Journal, 79*, 73–77.

Wang, K. Y., Liu, D. S., Tao, X. M., Zhang, J., Huppertz, T., Regenstein, J. M., et al. (2023). Decalcification strongly affects *in vitro* gastrointestinal digestion of bovine casein micelles under infant, adult and elderly conditions. *Food Hydrocolloids, 139*. Article 108515.

Wu, S. N., Li, G. T., Xue, Y., Ashokkumar, M., Zhao, H. B., Liu, D. S., et al. (2020). Solubilisation of micellar casein powders by high-power ultrasound. *Ultrasonics Sonochemistry, 67*. Article 105131.

Yahimi-Yazdi, S., Corredig, M., & Dalgleish, D. G. (2014). Studying the structure of β-casein-depleted bovine casein micelles using electron microscopy and fluorescent polyphenols. *Food Hydrocolloids, 42*, 171–177.

Yamauchi, K., Takemoto, S., & Tsugo, T. (1967). Calcium-binding property of dephosphorylated caseins. *Agricultural and Biological Chemistry, 31*, 54–63.

Yang, T. T., Liu, D. S., Tang, J., Tao, X. M., Zhang, J. L., Liu, X. M., et al. (2024). Formation of casein micelles simulating human milk casein composition from bovine caseins: Micellar structure and *in vitro* infant gastrointestinal digestion. *Food Hydrocolloids, 149*. Article 109610.

Yang, T. T., Liu, D. S., & Zhou, P. (2022). Temperature-dependent dissociation of human micellar β-casein: Implications of its phosphorylation degrees and casein micelle structures. *Food Chemistry, 376*. Article 131935.

Zhang, J. L., Liu, D. S., Tao, X. M., Tang, J., Peng, X. Y., Huppertz, T., et al. (2024). Effect of enzymatic dephosphorylation on caprine casein micelle structure. *Food Hydrocolloids, 148*. Article 109466.

Zou, Z. Z., Duley, J. A., Cowley, D. M., Reed, S., Arachchige, B. J., Koorts, P., et al. (2022). Digestibility of proteins in camel milk in comparison to bovine and human milk using an *in vitro* infant gastrointestinal digestion system. *Food Chemistry, 374*. Article 131704.